ACS Energy LETTERS

http://pubs.acs.org/journal/aelccp

An All-Fluorinated Ester Electrolyte for Stable High-Voltage Li Metal Batteries Capable of Ultra-Low-Temperature Operation

John Holoubek, Mingyu Yu, Sicen Yu, Minqian Li, Zhaohui Wu, Dawei Xia, Pranjal Bhaladhare, Matthew S. Gonzalez, Tod A. Pascal, Ping Liu, and Zheng Chen*

Cite This: ACS Energy Lett. 2020, 5, 1438−1447

Read Online

ACCESS | Metrics & More | Article Recommendations | Supporting Information

ABSTRACT: Improving the energy output of batteries at sub-zero temperatures is crucial to the long-term application of advanced electronics in extreme environments. This can generally be accomplished by employing high-voltage cathodes, applying Li metal anodes, and improving the electrolyte chemistry to provide facile kinetics at ultralow temperature. However, systems capable of all three of these have seldom been studied. Herein, we demonstrate the design of such a system through solvent fluorination, applying a 1 M $LiPF_6$ in a methyl 3,3,3-trifluoropionate (MTFP)/fluoroethylene carbonate (FEC) (9:1) electrolyte that simultaneously provided high-voltage cathode and Li metal anode reversibility at room temperature. This performance was attributed to the production of fluorine-rich interphases formed in the MTFP-based system, which was investigated by X-ray photoelectron spectroscopy (XPS). Furthermore, the all-fluorinated electrolyte provided 161, 149, and 133 mAh g^{-1} when discharged at −40, −50, and −60 °C, respectively, far exceeding the performance of the commercial electrolyte. This work provides new design principles for high-voltage batteries capable of ultra-low-temperature operation.

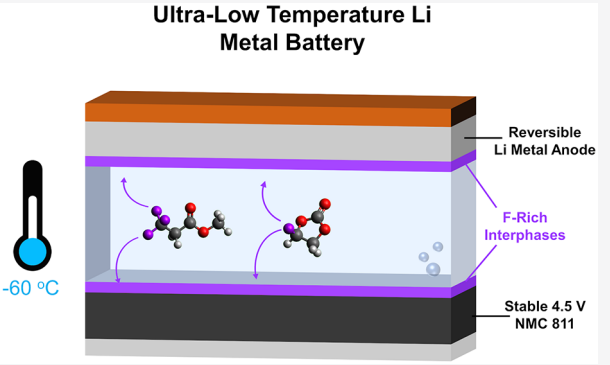

Lithium-ion batteries (LIBs) are a key technology for the operation of portable electronics in harsh environments such as high altitude and outer space. However, current LIBs are insufficient in terms of both energy density and the ability to retain such an energy density at temperatures below −20 °C, severely limiting their applications.[1−8]

To increase the baseline energy density of LIBs, it is crucial to employ Li metal anodes, which provide a theoretical capacity of 3860 mAh g^{-1} (vs 372 mAh g^{-1} in graphite), and to increase both the specific capacity and operating voltage of the cathode.[1,9] In particular, $LiNi_{0.8}Co_{0.1}Mn_{0.1}O_2$ (NMC 811) has been of primary interest due to its high but achievable operating window (≤4.5 V) and high capacity (>200 mAh g^{-1}),[10] yet despite these promising attributes, the long-term cycling stability is typically poor compared to those of cathodes with less Ni (e.g., $LiNi_{0.5}Co_{0.2}Mn_{0.3}O_2$ or NMC 523), which is generally a result of an increased level of parasitic electrolyte reactions at high voltages, an increased level of gas generation, and interfacial phase transformation.[11−14] These issues have been previously mitigated by lattice substitution/surface coatings[15−17] and advanced electrolyte formulations.[9,18−20] Li metal anodes face similar cycling stability issues, where the large volume change associated with metal conversion compounded with the inherently high reactivity of metallic Li often results in a low Coulombic efficiency (CE) during cycling, which fundamentally limits the cyclability of practical Li metal batteries (LMBs) due to the repeated consumption of cyclable Li^+.[21−23] These issues have been previously mitigated by designing advanced electrolytes,[20,24−29] constructing artificial Li surface coatings,[30−33] and applying porous three-dimensional hosts for Li deposition.[34−36]

On the contrary, common organic electrolytes exhibit notably sluggish charge transfer kinetics at low temperatures in addition to extremely reduced ionic conductivity, often freezing at temperatures below −20 °C. These factors result in significantly reduced cell output voltage and capacity.[2,8,37−49]

Received: March 22, 2020
Accepted: April 9, 2020
Published: April 9, 2020

https://dx.doi.org/10.1021/acsenergylett.0c00643
ACS Energy Lett. 2020, 5, 1438−1447

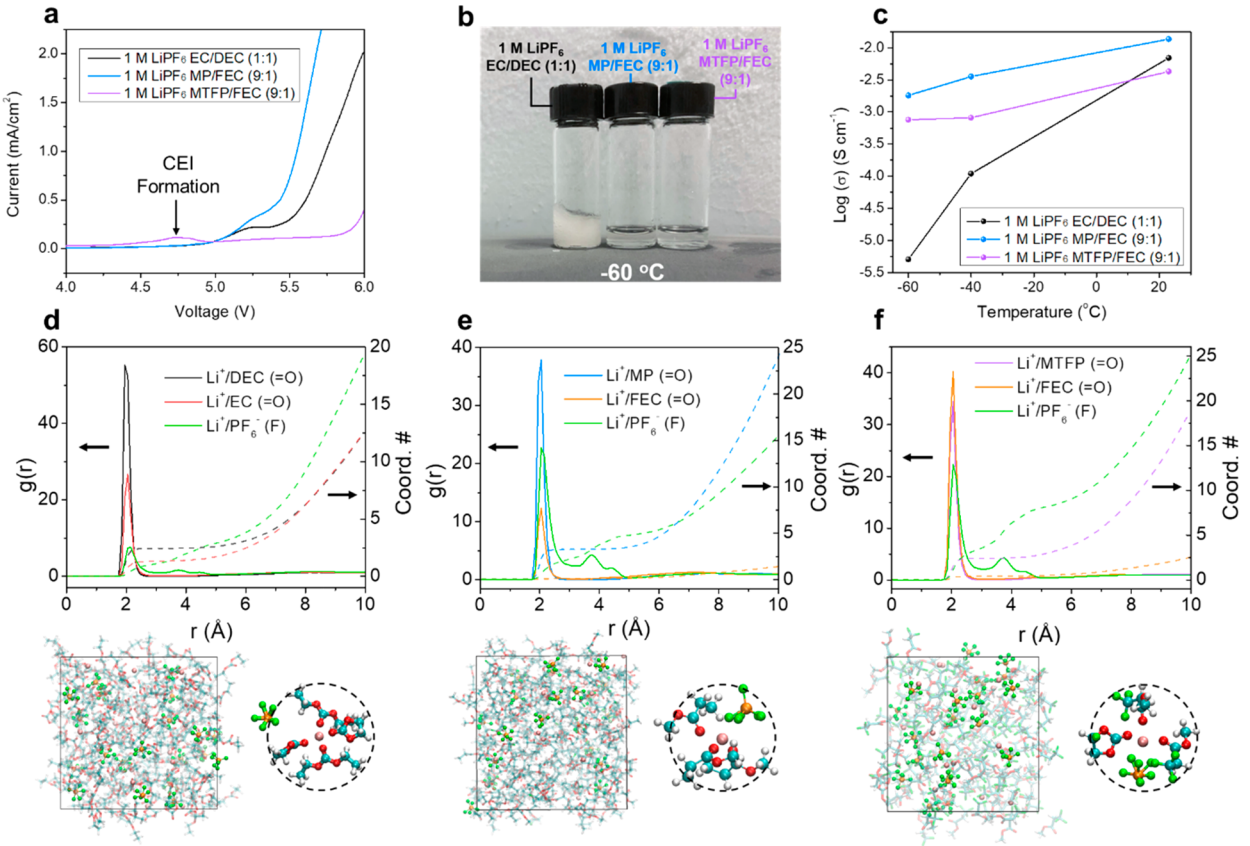

Figure 1. Properties of different electrolytes. (a) LSV profiles of conductive carbon electrodes in selected electrolytes at 1 mV s^{-1}. (b) Image of selected electrolytes at −60 °C. (c) Ionic conductivity of selected electrolytes measured at different temperatures. Li^+ radial distribution functions, snapshots, and representative solvation structures from MD simulations of (d) 1 M $LiPF_6$ EC/DEC (1:1), (e) 1 M $LiPF_6$ MP/FEC (9:1), and (f) 1 M $LiPF_6$ MTFP/FEC (9:1) electrolytes.

So far, traditional electrolyte chemistries have not been shown to support high-voltage cathodes for LMBs at extremely low temperatures. The poor energy retention of LIBs at low temperatures has generally been attributed to the internal resistances associated with Li^+ conduction through the bulk electrolyte, interfacial migration of Li^+ at the electrode interfaces, and Li^+ desolvation, which has been suggested to play an especially important role.[8,50−52] These resistances have been primarily addressed in previous studies through improvements in the battery electrolyte, employing novel salt additives,[37,38] and employing low-melting point[39−49] and/or low-polarizability[53−55] solvents with low viscosity. In spite of this progress, a system providing high energy retention at low temperatures and stable performance for high-voltage cathodes and Li metal anodes has yet to be reported to the best of our knowledge.

Herein, we propose and demonstrate a novel all-fluorinated carboxylate ester-based electrolyte that simultaneously provides stable long-term NMC 811 cycling at the high-voltage cutoff of 4.5 V and significantly improved Li metal deposition morphology and cycling efficiency, all while conserving the excellent low-temperature performance provided by nonfluorinated carboxylate ester-based systems.[39−42,50] In this work, we take a major step to achieve high-voltage LMBs that can be operated at ultralow temperatures through solvent fluorination, which is well-known to improve the oxidative stability of systems via the production of electrochemically stable fluorinated interphases.[9,20,24,55,56] This all-fluorinated ester system was found to provide an extremely stable NMC 811 capacity retention of 80% after 250 cycles with a cutoff voltage of 4.5 V, as well as superior Li metal performance, resulting in a practical Li (2-fold excess)||NMC811 full cell that provided 80 cycles of stable performance, long after comparable systems (nonfluorinated ester and carbonate) failed. In addition to its ability to support high-energy battery chemistries, the investigated electrolyte provided capacities of 161, 149, and 133 mAh g^{-1} when discharged at −40, −50, and −60 °C, respectively, a performance far superior to that of the standard carbonate control. We attribute this cycling stability to the fluorine-dominated interphases formed during cycling and the low-temperature performance to the physical properties of carboxylate ester solvents that yielded a high ionic conductivity of 0.75 mS cm^{-1} at −60 °C. This work provides a viable route for the future design of bifunctional electrolytes in support of stable high-voltage Li metal batteries at ultralow temperatures.

To provide a viable low-temperature control, methyl propionate (MP) was applied as the primary solvent with a 10% (v/v) fluoroethylene carbonate (FEC) additive and 1 M $LiPF_6$ salt to form an electrolyte system similar to that of our previous study, in which 10% FEC was found to be the minimum amount required to maintain electrochemical stability while providing improved low-temperature performance.[50] To further improve the electrochemical stability of this system for high-voltage applications, we substitute MP with its fluorinated counterpart, methyl 3,3,3-trifluoropionate (MTFP), which has been previously applied to high-voltage systems as a low-percentage additive.[57] The substitution of

https://dx.doi.org/10.1021/acsenergylett.0c00643
ACS Energy Lett. 2020, 5, 1438−1447

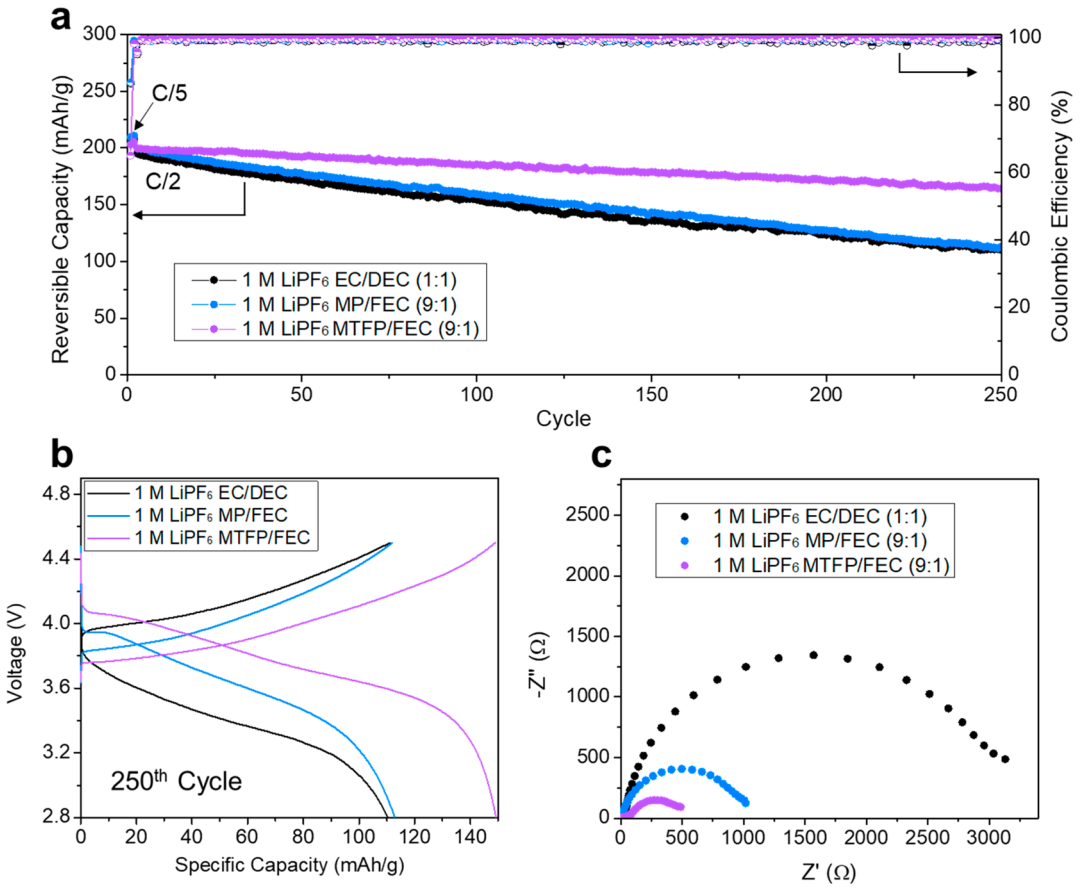

Figure 2. Room-temperature electrochemical behavior of selected electrolytes in NMC 811||Li half-cells. (a) Cycling performance at 0.5 C. (b) Voltage profiles at the 250th cycle. (c) Nyquist plots after cycling for 250 cycles at 0.5 C.

fluorine groups is well-known to decrease the HOMO energy of molecules due to the high ionic potential, high electronegativity, and low polarizability of the fluorine atom, resulting in an increased resistance to oxidation.[9,20,24,29,55−63] To preliminarily confirm the hypothesized electrolyte stability trends, linear scan voltammetry (LSV) measurements were carried out on conductive carbon electrodes (Supporting Information) to provide an accurate representation of performance in practical cells. As presented in Figure 1a, both 1 M $LiPF_6$ MP/FEC and 1 M $LiPF_6$ ethylene carbonate (EC)/diethyl carbonate (DEC) (1:1 volume) systems exhibit significant anodic current at ∼5.0 V versus Li/Li^+ (indicative of electrolyte decomposition), whereas the 1 M $LiPF_6$ MTFP/FEC system does not show the same behavior until ∼5.8 V. It is noteworthy that the MTFP-based electrolyte displays a small peak at ∼4.75 V, far before decomposition, which likely indicates the formation of a passivating CEI on the electrode surface. This trend was confirmed by gas phase, electronic structure calculations at the density functional theory (DFT) level of theory in Figure S1. We note, however, that such DFT calculations cannot inherently capture the complexity of decomposition mechanisms between the various system components in the multicomponent mixtures; however, such results do provide a qualitative indication of the onset of runaway oxidation in the systems of interest. In both electrolyte systems, we also note that the oxidative stability is further increased by the addition of 10% FEC, which is known to form passivating layers on both the anode side and the cathode side and yields a stability that is greater than those of the pure solvent systems (Figure S2).[9,18,29,50,55,64−70]

As previously stated, designing an electrolyte for ultra-low-temperature batteries requires the employment of solvents with a low melting point and a low viscosity, yielding a high ionic conductivity at low temperatures. As observed in Figure 1b, both ester-based electrolytes remain in a liquid state at −60 °C, while the typical carbonate electrolyte becomes frozen, indicating the higher melting points of carbonates compared to those of esters (Table S1). These observed trends are further substantiated by a comparison of the ionic conductivity of selected electrolytes with decreasing temperature measured via electrochemical impedance spectroscopy (EIS) in Figure 1c. It was found that 1 M $LiPF_6$ MTFP/FEC displayed a trend comparable to that of 1 M $LiPF_6$ MP/FEC, where the former retained an impressive ionic conductivity of 0.75 mS cm^{-1} at −60 °C, far exceeding that of 1 M $LiPF_6$ EC/DEC, which was found to decrease to 0.005 mS cm^{-1}.

To provide further insights into the solvation structure present in each electrolyte, classical molecular dynamics (MD) simulations were conducted as detailed in the Supporting Information. As displayed in Figure 1d, the radial distribution function of Li^+ in the 1 M $LiPF_6$ EC/DEC system displayed a characteristic solvent-separated ion pair (SSIP) structure, in which the Li^+ ions are primarily coordinated by solvent molecules (Li^+/solvent coordination number of 3.7), excluding PF_6^- to the secondary solvation shell. On the other hand, the MP/FEC and MTFP/FEC systems (Figure 1e,f) display a structure in which PF_6^- partially participates in the solvation,

https://dx.doi.org/10.1021/acsenergylett.0c00643
ACS Energy Lett. 2020, 5, 1438−1447

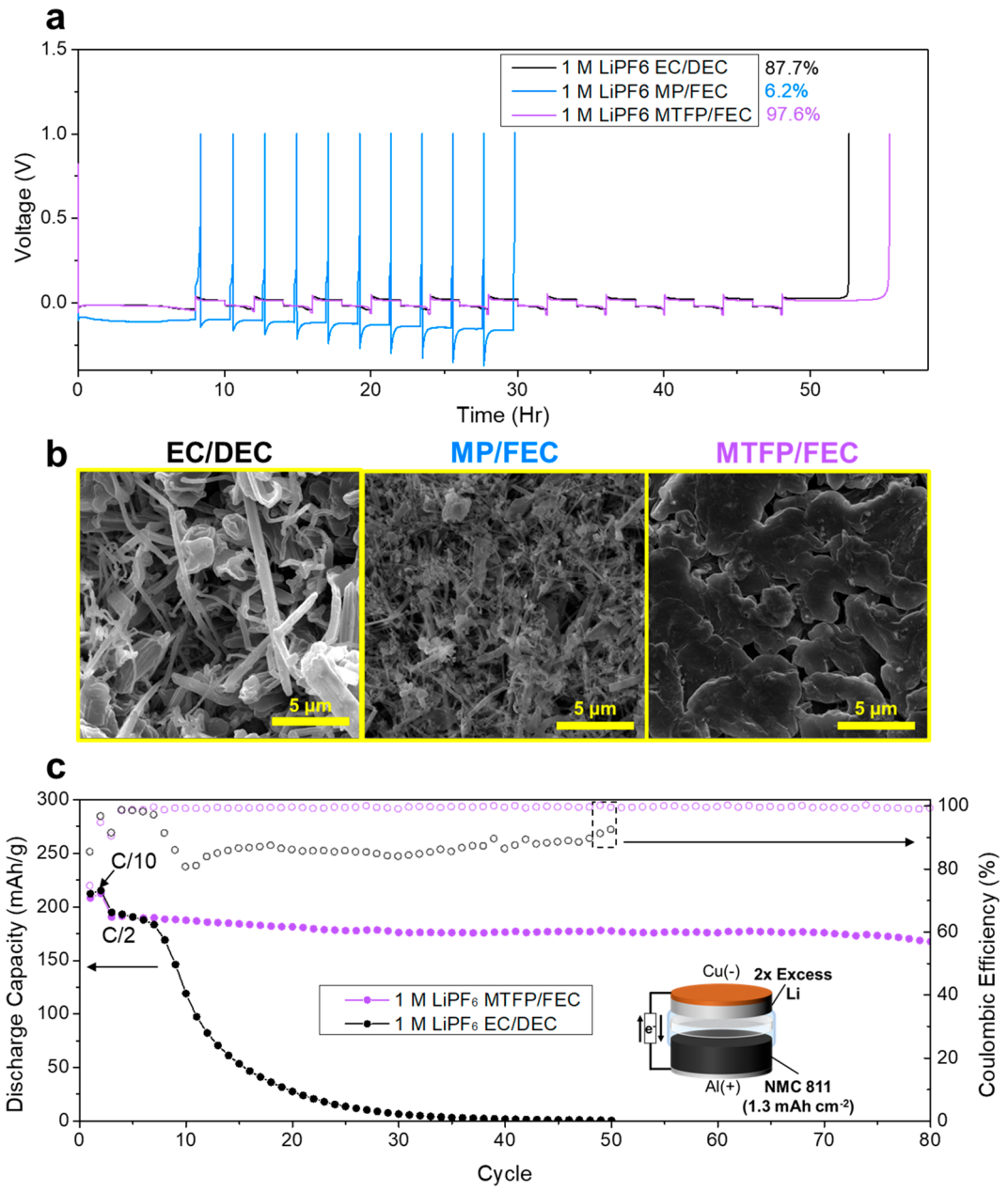

Figure 3. Room-temperature Li metal performance of selected electrolytes. (a) Coulombic efficiency measurements in Li||Cu cells according to the accurate measurement procedure.[79] (b) SEM images of 1 mAh cm^{-2} Li metal plated at 0.5 mA cm^{-2} in selected electrolytes. (c) Cycling performance of Li||NMC 811 full cells with a 2-fold excess Li capacity.

with calculated Li^+/solvent coordination numbers of 3.3, and 2.7, respectively. This configuration is similar to the contact ion pair (CIP) structure, which has commonly been observed in previous literature regarding electrolytes containing a high salt concentration, or low-polarizability solvents.[24,29,71−73] While this solvation structure is commonly associated with highly desirable properties, including a high Li^+ transference number and improved electrochemical stability at room temperature, the effect of this structure at low temperatures has not been studied to the best of our knowledge and will be studied further.[71,73]

It is well-known that typical commercial electrolytes, such as 1 M $LiPF_6$ EC/DEC, suffer parasitic reactions and oxidative decomposition at high voltages (typically >4.3 V), yielding corrosive species such as HF and organic deposits that are ineffective in protecting the cathode.[37,74−77] To test the practical stability of the MP- and MTFP-based electrolytes, we conducted cycling tests of NMC811||Li half-cells with an aggressive cutoff voltage of 4.5 V to exploit the high capacity of the nickel-rich cathode. As observed in Figure 2a, the cells in 1 M $LiPF_6$ MP/FEC and 1 M $LiPF_6$ EC/DEC both retain only 53% of their original capacity after 250 cycles, whereas the MTFP-based electrolyte provides a significantly improved capacity retention of 80% under the same conditions. Figure 2b displays the charge−discharge profiles of the 250th cycle of each cell employing selected electrolytes, where a significantly larger polarization and capacity degradation can be observed in the cell using the MP-based and carbonate-based electrolytes. These observations are likely a consequence of the oxidative decomposition of the electrolyte on the cathode surface.[9,58,78]

https://dx.doi.org/10.1021/acsenergylett.0c00643
ACS Energy Lett. 2020, 5, 1438−1447

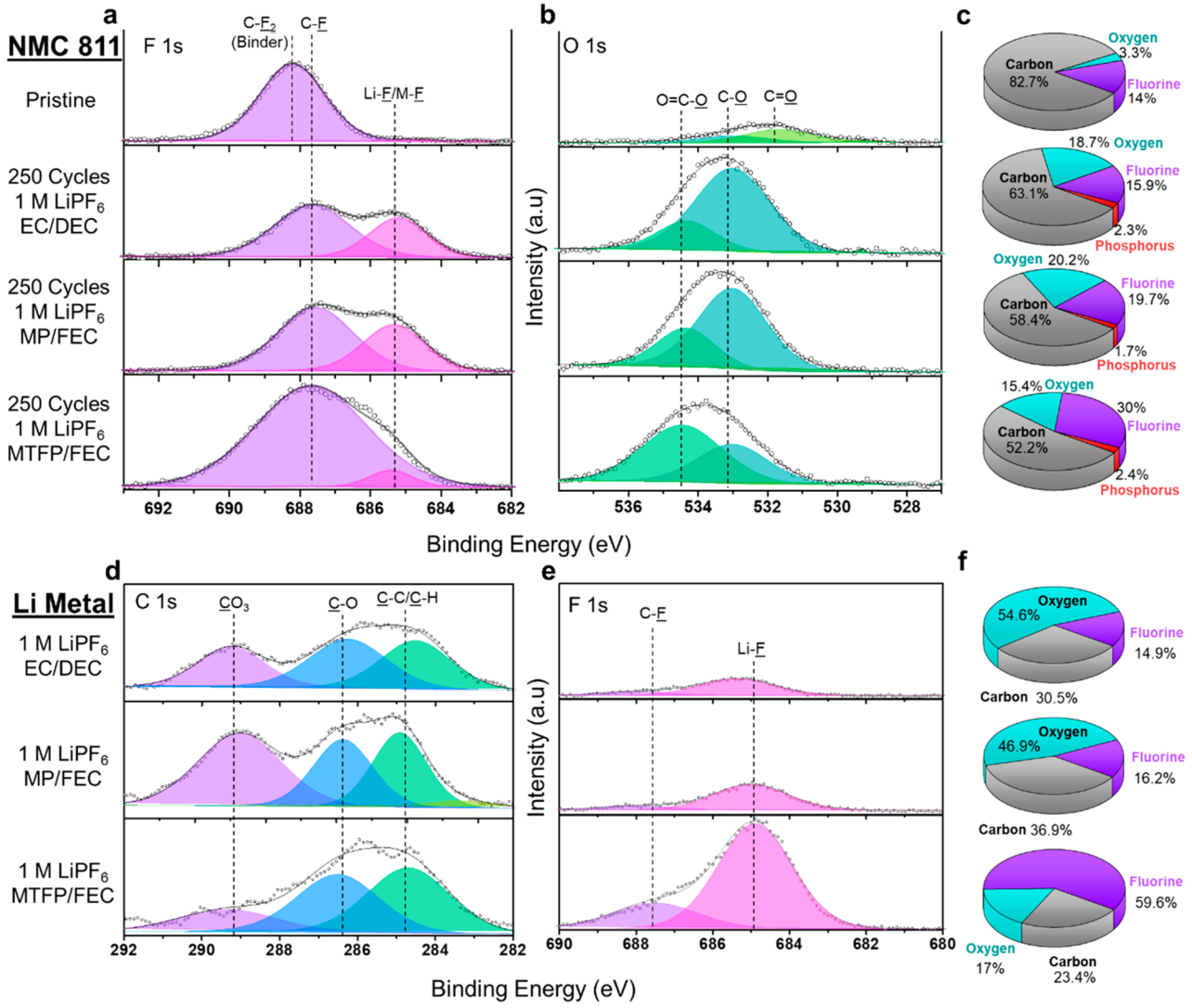

Figure 4. Characterization of electrode surfaces by XPS. (a) F 1s and (b) O 1s regions and (c) elemental composition of NMC 811 surfaces after 250 cycles. (d) C 1s and (e) F 1s regions and (f) elemental composition of 1 mAh cm^{-2} of plated Li.

For a deeper insight into this trend, EIS measurements were conducted on the cells after 250 cycles (Figure 2c), where the cell employing the MTFP-based electrolyte exhibits a charge transfer impedance (R_{ct}) significantly lower than that of the cell using a MP-based or carbonate-based electrolyte.

One feature of the MTFP-based electrolyte that is worth noting is the initial Coulombic efficiency (CE) of the first cycle, which ranks among the lowest of the investigated systems (60%, as opposed to ~85% for both 1 M $LiPF_6$ MP/FEC and 1 M $LiPF_6$ EC/DEC) before approaching 100% in the subsequent cycles. We attribute this to the formation of a robust CEI in the first cycle that serves to stabilize the long-term cycling of the cathode.

In addition to the long-term cycling stability of the cathode, a high Li metal CE is required for the application of high-voltage Li metal batteries. To measure this, we conducted testing with the commonly applied accurate CE measurement procedure developed by Adams et al.[79] to Li||Cu cells, which can be found in Figure 3a. We calculated that the MTFP/FEC system provided performance vastly superior to that of MP/FEC and EC/DEC electrolytes, exhibiting a CE of 97.6% compared to values of 6.2% and 87.7%, respectively. The morphologies associated with this vast divergence in CE were then examined via scanning electron microscopy (SEM) as shown in Figure 3b, where the EC/DEC and MP/FEC electrolytes were found to produce a highly dendritic Li structure, which is commonly found in similar systems with poor reductive stability.[20,24,29] The MTFP/FEC system, on the other hand, produced exceedingly large Li chunks without noticeable dendrites, which are typically associated with a small surface area and a low porosity and thus minimize decomposition reactions with the electrolyte.[20,22] Furthermore, these promising results were put to a more rigorous test, in which practical full cell LMBs were constructed with only a 2-fold excess of Li compared to NMC 811 (N/P = 2), which corresponds well to the goals set by the Battery 500 consortium.[1] This full cell was found to retain 88% capacity after 80 cycles, whereas the full cell employing 1 M $LiPF_6$ EC/DEC began to sharply degrade before 10 cycles had been performed (Figure 3c). Hence, it was determined that the MTFP/FEC electrolyte could provide remarkable stability for high-voltage Li metal batteries on both the cathode side and the anode side.

https://dx.doi.org/10.1021/acsenergylett.0c00643
ACS Energy Lett. 2020, 5, 1438−1447

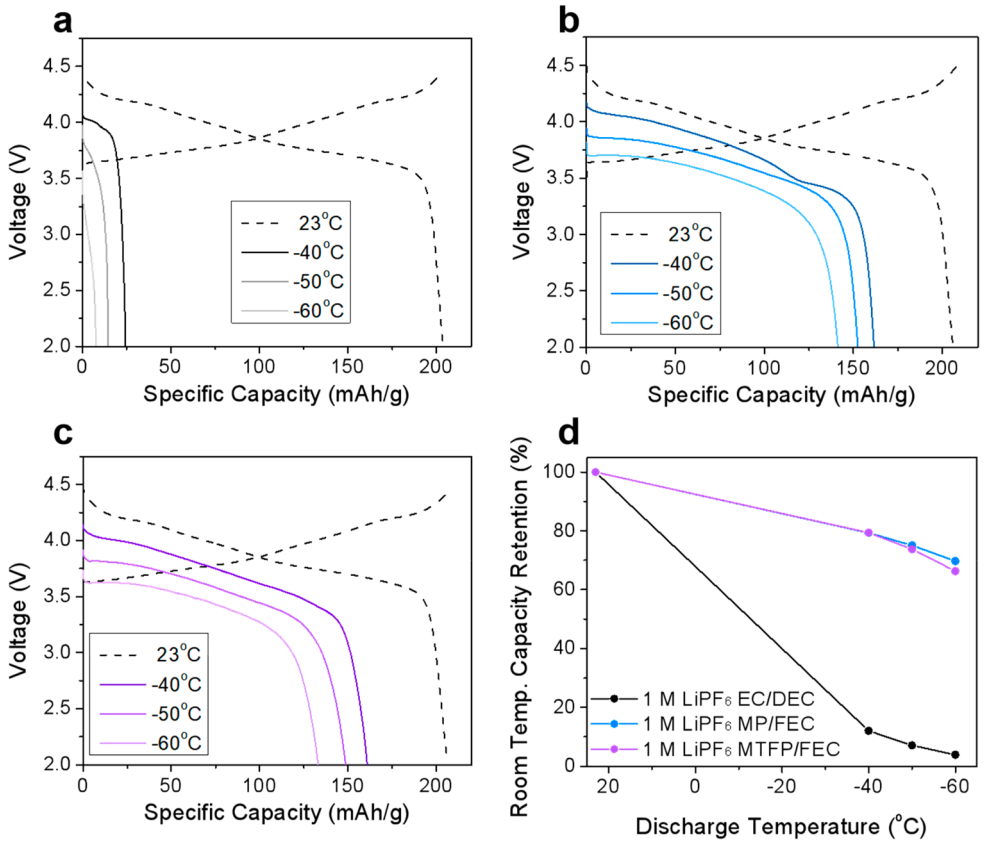

Figure 5. Low-temperature discharge behavior of selected electrolytes in NMC 811||Li half-cells at 0.1 C. Voltage profiles of NMC 811||Li cells in (a) 1 M $LiPF_6$ EC/DEC, (b) 1 M $LiPF_6$ MP/FEC, and (c) 1 M $LiPF_6$ MTFP/FEC. (d) Room-temperature capacity retention.

To further probe the interphases formed in each electrolyte, X-ray photoelectron spectroscopy (XPS) was applied to the NMC 811 cathodes before and after cycling, and the 1 mAh cm^{-2} of Li metal plated in each system. As observed in the comparison of C 1s spectra (Figure S5a), the overall intensity of the cycled cathodes decreases significantly and shifts toward organic oxygen species, indicating the presence of the CEI after cycling. Comparison of the F 1s spectra (Figure 4a) indicates two primary fluorine-based CEI components: Li−F/M−F (~685.3 eV), which is typically a product of the decomposition of $LiPF_6$ and or FEC (when applicable), and C−F (~687.7 eV), which is likely a product of similar salt/solvent decomposition reactions.[9,78] While little deviation can be observed in the F 1s spectra between cathodes cycled in carbonate and MP-based electrolytes, the MTFP-based electrolyte yields a CEI clearly dominated by C−F. Organic fluoride dominant CEI compositions are rarely observed in the literature;[9,20,53,78,80,81] however, we believe such an interface is responsible for the highly stable performance provided by the MTFP/FEC system. Further comparison with the O 1s spectra found in Figure 4b reveals an increased presence of O−C═O (~534.4 eV), which may suggest that the CEI primarily consists of fluorinated polyesters. Quantitative analysis of the XPS results (Figure 4c) further confirms a higher atomic fluorine content and a lower content of carbon overall in the NMC 811 CEI after cycling in the 1 M $LiPF_6$ MTFP/FEC system. The atomic fluorine percentages for the MTFP/FEC, MP/FEC, and EC/DEC electrolyte system are 30%, 19.7%, and 15.9%, respectively, while the corresponding atomic carbon contents are 52.2%, 58.4%, and 63.1%, respectively. Furthermore, this high fluorine content was observed to be uniformly distributed through the NMC 811 particle, as shown in Figure S6.

The XPS profiles of the solid electrolyte interphase (SEI) on plated Li of each electrolyte show a similar trend. First, we observed a substantial decrease in the overall level of carbon found in the MTFP system, primarily due to the reduced CO_3^{2-} peak as shown in Figure 4d. Most importantly, we note the extreme increase in the level of Li−F on the surface of plated Li in the MTFP/FEC system (Figure 4e), where the overall fluorine content was found to be 59.6%, as compared to the values of 16.2% and 14.9% found in the MP/FEC and EC/DEC electrolytes, respectively (Figure 4f). Li−F is known to be particularly desirable as a SEI component for Li metal anodes, due to its electrochemical stability and its strong correlation to systems providing a high cycling CE.[22−29,55,56] Hence, we believe highly fluorinated interphases result in both the stable cycling of NMC 811 at high voltages and the high CE of Li metal plating demonstrated by the MTFP/FEC electrolyte.

To demonstrate the advantage of the designed ester electrolytes at low temperatures, NMC 811||Li half-cells were tested using a method commonly applied in low-temperature battery studies, in which the cells were charged at room temperature followed by discharge at low temperatures to simulate practical device applications (Supporting Information).[2,8,39,40,47,50] Although the origins of low-temperature performance degradation remain controversial, the primary limiting factors are generally believed to be the reduced bulk ionic conductivity of the electrolyte and a severe reduction in charge transfer kinetics, which has been suggested to be dominated by Li^+ desolvation.[2−8,39−48,50,51] In terms of these

https://dx.doi.org/10.1021/acsenergylett.0c00643
ACS Energy Lett. 2020, 5, 1438−1447

metrics, we believe our ester electrolytes are superior in every respect, owing to the high retention of ionic conductivity at ultralow temperatures and the introduction of FEC, which has been noted to have a Li^+ solvation energy significantly lower than that of EC, allowing for facile desolvation.[55]

The voltage profiles of these tests are displayed in Figure 5a−c, and the retention versus temperature for each system is summarized in Figure 5d. From these data, we observe that the typical carbonate electrolyte was unable to support the low-temperature operation of the cell, failing to offer any significant capacity (∼10%) at −40 °C due to the high melting point of EC/DEC, as well as the strong binding between Li^+ and EC.[55,82−84] By contrast, the ester electrolytes made remarkable progress in enhancing low-temperature device performance, where the MP/FEC system provided room-temperature capacity retention of 79.4%, 75.0%, and 69.7% at −40, −50, and −60 °C, respectively, which corresponds well to the cathode impedance trends shown in Figure S8. While the MTFP/FEC system provided slightly reduced retention of 73.7% and 66.2% at −50 and −60 °C, respectively, the relatively small discrepancy is likely due to the reduced ionic conductivity of the MTFP/FEC system. Despite this, the significantly improved stability of the NMC811 cathode at high voltages in addition to its vastly improved Li metal performance indicates the clear superiority of the MTFP/FEC system, in which the baseline energy density of the battery can be improved while conserving remarkable capacity retention at ultralow temperatures.

In summary, we have developed a novel all-fluorinated carboxylate ester-based electrolyte for LIBs, which was found to simultaneously provide high capacity retention at ultralow temperatures, remarkable oxidative stability in support of high-voltage, nickel-rich cathodes, and high-efficiency Li metal cycling with a homogeneous deposition morphology. Specifically, employing 1 M $LiPF_6$ in MTFP/FEC (9:1 volume ratio) yielded a capacity retention of 80% for NMC 811||Li half-cells charged to 4.5 V after 250 cycles, whereas the analogous 1 M $LiPF_6$ in MP/FEC (9:1) and 1 M $LiPF_6$ in EC/DEC (1:1) provided a retention of only 53% under the same conditions. On the anode side, the MTFP/FEC system provided a Li metal CE of 97.6%, compared to the values of 6.2% and 87.7% found in the MP/FEC and EC/DEC systems, respectively, which produced a 2-fold excess Li||NMC 811 full cell that retained 88% of its capacity after 80 cycles. This remarkable stability was attributed to the highly fluorinated interphases produced by the MTFP/FEC system found on both the cathode side and the anode side. At ultralow temperatures, the MTFP/FEC system was also found to produce performance comparable to that of the MP/FEC system, which has been previously noted for its remarkable performance at low temperatures, retaining 161, 149, and 133 mAh g^{-1} when discharged at −40, −50, and −60 °C, respectively, at a rate of 0.1 C. In the future, further exploration of novel electrolyte components and high-voltage cathode chemistries may prove to be crucial to the future of portable electronics in extremely cold environments. This work provides an early route to enabling high-voltage, nickel-rich cathode LMBs at ultralow temperatures.

■ ASSOCIATED CONTENT

Supporting Information

The Supporting Information is available free of charge at https://pubs.acs.org/doi/10.1021/acsenergylett.0c00643.

Experimental and computational methods, table of physical properties of organic solvents, DFT and electrolyte stability data, voltage profiles of NMC 811|| Li half-cells, rate performance, XPS spectra, and *ex situ* XRD patterns (PDF)

■ AUTHOR INFORMATION

Corresponding Author

Zheng Chen − *Department of NanoEngineering, Program of Materials Science, Program of Chemical Engineering, and Sustainable Power and Energy Center, University of California, San Diego, La Jolla, California 92093, United States;* orcid.org/0000-0002-9186-4298; Email: zhengchen@eng.ucsd.edu

Authors

John Holoubek − *Department of NanoEngineering, University of California, San Diego, La Jolla, California 92093, United States*

Mingyu Yu − *Program of Materials Science, University of California, San Diego, La Jolla, California 92093, United States*

Sicen Yu − *Program of Materials Science, University of California, San Diego, La Jolla, California 92093, United States*

Minqian Li − *Program of Chemical Engineering, University of California, San Diego, La Jolla, California 92093, United States*

Zhaohui Wu − *Program of Chemical Engineering, University of California, San Diego, La Jolla, California 92093, United States*

Dawei Xia − *Department of NanoEngineering, University of California, San Diego, La Jolla, California 92093, United States*

Pranjal Bhaladhare − *Department of NanoEngineering, University of California, San Diego, La Jolla, California 92093, United States*

Matthew S. Gonzalez − *Department of NanoEngineering, University of California, San Diego, La Jolla, California 92093, United States*

Tod A. Pascal − *Department of NanoEngineering and Program of Chemical Engineering, University of California, San Diego, La Jolla, California 92093, United States*

Ping Liu − *Department of NanoEngineering, Program of Materials Science, Program of Chemical Engineering, and Sustainable Power and Energy Center, University of California, San Diego, La Jolla, California 92093, United States;* orcid.org/0000-0002-1488-1668

Complete contact information is available at: https://pubs.acs.org/10.1021/acsenergylett.0c00643

Author Contributions

J.H. and M.Y. contributed equally. J.H. conceived the original idea and initial experimental plan. Z.C. directed the project. J.H. and M.Y. carried out the experiments. S.Y., M.L., Z.W., and M.S.G. assisted with characterization. J.H., Z.C., and M.Y. wrote the paper. All authors discussed the results and commented on the manuscript.

Notes

The authors declare no competing financial interest.

■ ACKNOWLEDGMENTS

This work was supported by an Early Career Faculty grant from NASA's Space Technology Research Grants Program (ECF 80NSSC18K1512) to Z.C. P.L. and Z.C. acknowledge the start-up fund from the Jacob School of Engineering at the University of California, San Diego (UCSD). A majority of cell

fabrication and electrochemical testing was performed in the UCSD-MTI Battery Fabrication and the UCSD-Arbin Battery Testing Facility. This work was performed in part at the San Diego Nanotechnology Infrastructure (SDNI) of UCSD, a member of the National Nanotechnology Coordinated Infrastructure, which is supported by the National Science Foundation (Grant ECCS-1542148).

REFERENCES

(1) Liu, J.; Bao, Z.; Cui, Y.; Dufek, E. J.; Goodenough, J. B.; Khalifah, P.; Li, Q.; Liaw, B. Y.; Liu, P.; Manthiram, A.; Meng, Y. S.; Subramanian, V. R.; Toney, M. F.; Viswanathan, V. V.; Whittingham, M. S.; Xiao, J.; Xu, W.; Yang, J.; Yang, X.-Q.; Zhang, J.-G. Pathways for Practical High-Energy Long-Cycling Lithium Metal Batteries. *Nat. Energy* **2019**, *4* (3), 180−186.

(2) Zhang, S. S.; Xu, K.; Jow, T. R. The Low Temperature Performance of Li-Ion Batteries. *J. Power Sources* **2003**, *115* (1), 137−140.

(3) Smart, M. C.; Ratnakumar, B. V.; Ewell, R. C.; Surampudi, S.; Puglia, F. J.; Gitzendanner, R. The Use of Lithium-Ion Batteries for JPL's Mars Missions. *Electrochim. Acta* **2018**, *268*, 27−40.

(4) Jaguemont, J.; Boulon, L.; Dubé, Y. A Comprehensive Review of Lithium-Ion Batteries Used in Hybrid and Electric Vehicles at Cold Temperatures. *Appl. Energy* **2016**, *164*, 99−114.

(5) Huang, C.-K.; Sakamoto, J. S.; Wolfenstine, J.; Surampudi, S. The Limits of Low-Temperature Performance of Li-Ion Cells. *J. Electrochem. Soc.* **2000**, *147* (8), 2893−2896.

(6) Zhu, G.; Wen, K.; Lv, W.; Zhou, X.; Liang, Y.; Yang, F.; Chen, Z.; Zou, M.; Li, J.; Zhang, Y.; He, W. Materials Insights into Low-Temperature Performances of Lithium-Ion Batteries. *J. Power Sources* **2015**, *300*, 29−40.

(7) Zhang, S. S.; Xu, K.; Jow, T. R. Low Temperature Performance of Graphite Electrode in Li-Ion Cells. *Electrochim. Acta* **2002**, *48* (3), 241−246.

(8) Li, Q.; Lu, D.; Zheng, J.; Jiao, S.; Luo, L.; Wang, C.-M.; Xu, K.; Zhang, J.-G.; Xu, W. Li+-Desolvation Dictating Lithium-Ion Battery's Low-Temperature Performances. *ACS Appl. Mater. Interfaces* **2017**, *9* (49), 42761−42768.

(9) Fan, X.; Chen, L.; Borodin, O.; Ji, X.; Chen, J.; Hou, S.; Deng, T.; Zheng, J.; Yang, C.; Liou, S.-C.; Amine, K.; Xu, K.; Wang, C. Non-Flammable Electrolyte Enables Li-Metal Batteries with Aggressive Cathode Chemistries. *Nat. Nanotechnol.* **2018**, *13* (8), 715.

(10) Li, W.; Song, B.; Manthiram, A. High-Voltage Positive Electrode Materials for Lithium-Ion Batteries. *Chem. Soc. Rev.* **2017**, *46* (10), 3006−3059.

(11) Li, J.; Downie, L. E.; Ma, L.; Qiu, W.; Dahn, J. R. Study of the Failure Mechanisms of $LiNi_{0.8}Mn_{0.1}Co_{0.1}O_2$ Cathode Material for Lithium Ion Batteries. *J. Electrochem. Soc.* **2015**, *162* (7), A1401−A1408.

(12) Bak, S.-M.; Hu, E.; Zhou, Y.; Yu, X.; Senanayake, S. D.; Cho, S.-J.; Kim, K.-B.; Chung, K. Y.; Yang, X.-Q.; Nam, K.-W. Structural Changes and Thermal Stability of Charged $LiNi_xMn_yCo_zO_2$ Cathode Materials Studied by Combined In Situ Time-Resolved XRD and Mass Spectroscopy. *ACS Appl. Mater. Interfaces* **2014**, *6* (24), 22594−22601.

(13) Li, T.; Yuan, X.-Z.; Zhang, L.; Song, D.; Shi, K.; Bock, C. Degradation Mechanisms and Mitigation Strategies of Nickel-Rich NMC-Based Lithium-Ion Batteries. *Electrochem. Energy Rev.* **2020**, *3*, 43−80.

(14) Li, H.; Liu, A.; Zhang, N.; Wang, Y.; Yin, S.; Wu, H.; Dahn, J. R. An Unavoidable Challenge for Ni-Rich Positive Electrode Materials for Lithium-Ion Batteries. *Chem. Mater.* **2019**, *31* (18), 7574−7583.

(15) Yang, J.; Xia, Y. Suppressing the Phase Transition of the Layered Ni-Rich Oxide Cathode during High-Voltage Cycling by Introducing Low-Content Li_2MnO_3. *ACS Appl. Mater. Interfaces* **2016**, *8* (2), 1297−1308.

(16) Xin, F.; Zhou, H.; Chen, X.; Zuba, M.; Chernova, N.; Zhou, G.; Whittingham, M. S. Li−Nb−O Coating/Substitution Enhances the Electrochemical Performance of the $LiNi_{0.8}Mn_{0.1}Co_{0.1}O_2$ (NMC 811) Cathode. *ACS Appl. Mater. Interfaces* **2019**, *11* (38), 34889−34894.

(17) Xie, J.; Sendek, A. D.; Cubuk, E. D.; Zhang, X.; Lu, Z.; Gong, Y.; Wu, T.; Shi, F.; Liu, W.; Reed, E. J.; Cui, Y. Atomic Layer Deposition of Stable LiAlF4 Lithium Ion Conductive Interfacial Layer for Stable Cathode Cycling. *ACS Nano* **2017**, *11* (7), 7019−7027.

(18) Li, J.; Liu, H.; Xia, J.; Cameron, A. R.; Nie, M.; Botton, G. A.; Dahn, J. R. The Impact of Electrolyte Additives and Upper Cut-off Voltage on the Formation of a Rocksalt Surface Layer in $LiNi_{0.8}Mn_{0.1}Co_{0.1}O_2$ Electrodes. *J. Electrochem. Soc.* **2017**, *164* (4), A655−A665.

(19) Tatara, R.; Yu, Y.; Karayaylali, P.; Chan, A. K.; Zhang, Y.; Jung, R.; Maglia, F.; Giordano, L.; Shao-Horn, Y. Enhanced Cycling Performance of Ni-Rich Positive Electrodes (NMC) in Li-Ion Batteries by Reducing Electrolyte Free-Solvent Activity. *ACS Appl. Mater. Interfaces* **2019**, *11* (38), 34973−34988.

(20) Ren, X.; Zou, L.; Cao, X.; Engelhard, M. H.; Liu, W.; Burton, S. D.; Lee, H.; Niu, C.; Matthews, B. E.; Zhu, Z.; Wang, C.; Arey, B. W.; Xiao, J.; Liu, J.; Zhang, J.-G.; Xu, W. Enabling High-Voltage Lithium-Metal Batteries under Practical Conditions. *Joule* **2019**, *3* (7), 1662−1676.

(21) Xu, W.; Wang, J.; Ding, F.; Chen, X.; Nasybulin, E.; Zhang, Y.; Zhang, J.-G. Lithium MetalAnodes for Rechargeable Batteries. *Energy Environ. Sci.* **2014**, *7* (2), 513−537.

(22) Li, S.; Jiang, M.; Xie, Y.; Xu, H.; Jia, J.; Li, J. Developing High-Performance Lithium Metal Anode in Liquid Electrolytes: Challenges and Progress. *Adv. Mater.* **2018**, *30* (17), 1706375.

(23) Lin, D.; Liu, Y.; Cui, Y. Reviving the Lithium Metal Anode for High-Energy Batteries. *Nat. Nanotechnol.* **2017**, *12* (3), 194−206.

(24) Chen, S.; Zheng, J.; Mei, D.; Han, K. S.; Engelhard, M. H.; Zhao, W.; Xu, W.; Liu, J.; Zhang, J.-G. High-Voltage Lithium-Metal Batteries Enabled by Localized High-Concentration Electrolytes. *Adv. Mater.* **2018**, *30* (21), 1706102.

(25) Qian, J.; Henderson, W. A.; Xu, W.; Bhattacharya, P.; Engelhard, M.; Borodin, O.; Zhang, J.-G. High Rate and Stable Cycling of Lithium Metal Anode. *Nat. Commun.* **2015**, *6*, 6362.

(26) Alvarado, J.; Schroeder, M. A.; Pollard, T. P.; Wang, X.; Lee, J. Z.; Zhang, M.; Wynn, T.; Ding, M.; Borodin, O.; Meng, Y. S.; Xu, K. Bisalt Ether Electrolytes: A Pathway towards Lithium Metal Batteries with Ni-Rich Cathodes. *Energy Environ. Sci.* **2019**, *12* (2), 780−794.

(27) Ren, X.; Zou, L.; Jiao, S.; Mei, D.; Engelhard, M. H.; Li, Q.; Lee, H.; Niu, C.; Adams, B. D.; Wang, C.; Liu, J.; Zhang, J.-G.; Xu, W. High-Concentration Ether Electrolytes for Stable High-Voltage Lithium Metal Batteries. *ACS Energy Lett.* **2019**, *4* (4), 896−902.

(28) Cao, X.; Ren, X.; Zou, L.; Engelhard, M. H.; Huang, W.; Wang, H.; Matthews, B. E.; Lee, H.; Niu, C.; Arey, B. W.; Cui, Y.; Wang, C.; Xiao, J.; Liu, J.; Xu, W.; Zhang, J.-G. Monolithic Solid−Electrolyte Interphases Formed in Fluorinated Orthoformate-Based Electrolytes Minimize Li Depletion and Pulverization. *Nat. Energy* **2019**, *4* (9), 796−805.

(29) Suo, L.; Xue, W.; Gobet, M.; Greenbaum, S. G.; Wang, C.; Chen, Y.; Yang, W.; Li, Y.; Li, J. Fluorine-Donating Electrolytes Enable Highly Reversible 5-V-Class Li Metal Batteries. *Proc. Natl. Acad. Sci. U. S. A.* **2018**, *115* (6), 1156−1161.

(30) Zhou, H.; Yu, S.; Liu, H.; Liu, P. Protective Coatings for Lithium Metal Anodes: Recent Progress and Future Perspectives. *J. Power Sources* **2020**, *450*, 227632.

(31) Li, N.-W.; Yin, Y.-X.; Yang, C.-P.; Guo, Y.-G. An Artificial Solid Electrolyte Interphase Layer for Stable Lithium Metal Anodes. *Adv. Mater.* **2016**, *28* (9), 1853−1858.

(32) Wang, G.; Xiong, X.; Xie, D.; Fu, X.; Lin, Z.; Yang, C.; Zhang, K.; Liu, M. A Scalable Approach for Dendrite-Free Alkali Metal Anodes via Room-Temperature Facile Surface Fluorination. *ACS Appl. Mater. Interfaces* **2019**, *11* (5), 4962−4968.

(33) Liang, X.; Pang, Q.; Kochetkov, I. R.; Sempere, M. S.; Huang, H.; Sun, X.; Nazar, L. F. A Facile Surface Chemistry Route to a Stabilized Lithium Metal Anode. *Nat. Energy* **2017**, *2* (9), 17119.

(34) Ke, X.; Liang, Y.; Ou, L.; Liu, H.; Chen, Y.; Wu, W.; Cheng, Y.; Guo, Z.; Lai, Y.; Liu, P.; Shi, Z. Surface Engineering of Commercial

https://dx.doi.org/10.1021/acsenergylett.0c00643
ACS Energy Lett. 2020, 5, 1438−1447

Ni Foams for Stable Li Metal Anodes. *Energy Storage Mater.* **2019**, *23*, 547−555.
(35) Niu, C.; Pan, H.; Xu, W.; Xiao, J.; Zhang, J.-G.; Luo, L.; Wang, C.; Mei, D.; Meng, J.; Wang, X.; Liu, Z.; Mai, L.; Liu, J. Self-Smoothing Anode for Achieving High-Energy Lithium Metal Batteries under Realistic Conditions. *Nat. Nanotechnol.* **2019**, *14* (6), 594−601.
(36) Liu, H.; Yue, X.; Xing, X.; Yan, Q.; Huang, J.; Petrova, V.; Zhou, H.; Liu, P. A Scalable 3D Lithium Metal Anode. *Energy Storage Mater.* **2019**, *16*, 505−511.
(37) Liao, B.; Li, H.; Xu, M.; Xing, L.; Liao, Y.; Ren, X.; Fan, W.; Yu, L.; Xu, K.; Li, W. Designing Low Impedance Interface Films Simultaneously on Anode and Cathode for High Energy Batteries. *Adv. Energy Mater.* **2018**, *8* (22), 1800802.
(38) Zhang, S. S.; Xu, K.; Jow, T. R. A New Approach toward Improved Low Temperature Performance of Li-Ion Battery. *Electrochem. Commun.* **2002**, *4* (11), 928−932.
(39) Smart, M. C.; Ratnakumar, B. V.; Chin, K. B.; Whitcanack, L. D. Lithium-Ion Electrolytes Containing Ester Cosolvents for Improved Low Temperature Performance. *J. Electrochem. Soc.* **2010**, *157* (12), A1361−A1374.
(40) Zhang, S. S.; Xu, K.; Jow, T. R. Low Temperature Performance of Graphite Electrode in Li-Ion Cells. *Electrochim. Acta* **2002**, *48* (3), 241−246.
(41) Smart, M. C.; Lucht, B. L.; Dalavi, S.; Krause, F. C.; Ratnakumar, B. V. The Effect of Additives upon the Performance of MCMB/$LiNi_xCo_{1-x}O_2$ Li-Ion Cells Containing Methyl Butyrate-Based Wide Operating Temperature Range Electrolytes. *J. Electrochem. Soc.* **2012**, *159* (6), A739−A751.
(42) Smart, M. C.; Ratnakumar, B. V.; Behar, A.; Whitcanack, L. D.; Yu, J.-S.; Alamgir, M. Gel Polymer Electrolyte Lithium-Ion Cells with Improved Low Temperature Performance. *J. Power Sources* **2007**, *165* (2), 535−543.
(43) Smart, M. C.; Ratnakumar, B. V.; Surampudi, S. Electrolytes for Low-Temperature Lithium Batteries Based on Ternary Mixtures of Aliphatic Carbonates. *J. Electrochem. Soc.* **1999**, *146* (2), 486−492.
(44) Plichta, E. J.; Hendrickson, M.; Thompson, R.; Au, G.; Behl, W. K.; Smart, M. C.; Ratnakumar, B. V.; Surampudi, S. Development of Low Temperature Li-Ion Electrolytes for NASA and DoD Applications. *J. Power Sources* **2001**, *94* (2), 160−162.
(45) Logan, E. R.; Tonita, E. M.; Gering, K. L.; Li, J.; Ma, X.; Beaulieu, L. Y.; Dahn, J. R. A Study of the Physical Properties of Li-Ion Battery Electrolytes Containing Esters. *J. Electrochem. Soc.* **2018**, *165* (2), A21−A30.
(46) Plichta, E. J.; Behl, W. K. A Low-Temperature Electrolyte for Lithium and Lithium-Ion Batteries. *J. Power Sources* **2000**, *88* (2), 192−196.
(47) Li, Q.; Jiao, S.; Luo, L.; Ding, M. S.; Zheng, J.; Cartmell, S. S.; Wang, C.-M.; Xu, K.; Zhang, J.-G.; Xu, W. Wide-Temperature Electrolytes for Lithium-Ion Batteries. *ACS Appl. Mater. Interfaces* **2017**, *9* (22), 18826−18835.
(48) Dong, X.; Guo, Z.; Guo, Z.; Wang, Y.; Xia, Y. Organic Batteries Operated at − 70°C. *Joule* **2018**, *2* (5), 902−913.
(49) Dong, X.; Lin, Y.; Li, P.; Ma, Y.; Huang, J.; Bin, D.; Wang, Y.; Qi, Y.; Xia, Y. High-Energy Rechargeable Metallic Lithium Battery at − 70 °C Enabled by a Cosolvent Electrolyte. *Angew. Chem., Int. Ed.* **2019**, *58* (17), 5623−5627.
(50) Holoubek, J.; Yin, Y.; Li, M.; Yu, M.; Meng, Y. S.; Liu, P.; Chen, Z. Exploiting Mechanistic Solvation Kinetics for Dual-Graphite Batteries with High Power Output at Extremely Low Temperature. *Angew. Chem., Int. Ed.* **2019**, *58* (52), 18892−18897.
(51) Xu, K.; von Cresce, A.; Lee, U. Differentiating Contributions to "Ion Transfer" Barrier from Interphasial Resistance and Li^+ Desolvation at Electrolyte/Graphite Interface. *Langmuir* **2010**, *26* (13), 11538−11543.
(52) Xu, K. Charge-Transfer" Process at Graphite/Electrolyte Interface and the Solvation Sheath Structure of Li^+ in Nonaqueous Electrolytes. *J. Electrochem. Soc.* **2007**, *154* (3), A162.
(53) Rustomji, C. S.; Yang, Y.; Kim, T. K.; Mac, J.; Kim, Y. J.; Caldwell, E.; Chung, H.; Meng, Y. S. Liquefied Gas Electrolytes for Electrochemical Energy Storage Devices. *Science* **2017**, *356* (6345), No. eaal4263.
(54) Yang, Y.; Davies, D. M.; Yin, Y.; Borodin, O.; Lee, J. Z.; Fang, C.; Olguin, M.; Zhang, Y.; Sablina, E. S.; Wang, X.; Rustomji, C. S.; Meng, Y. S. High-Efficiency Lithium-Metal Anode Enabled by Liquefied Gas Electrolytes. *Joule* **2019**, *3* (8), 1986−2000.
(55) Fan, X.; Ji, X.; Chen, L.; Chen, J.; Deng, T.; Han, F.; Yue, J.; Piao, N.; Wang, R.; Zhou, X.; Xiao, X.; Chen, L.; Wang, C. All-Temperature Batteries Enabled by Fluorinated Electrolytes with Non-Polar Solvents. *Nat. Energy* **2019**, *4* (10), 882−890.
(56) Niu, C.; Lee, H.; Chen, S.; Li, Q.; Du, J.; Xu, W.; Zhang, J.-G.; Whittingham, M. S.; Xiao, J.; Liu, J. High-Energy Lithium Metal Pouch Cells with Limited Anode Swelling and Long Stable Cycles. *Nat. Energy* **2019**, *4* (7), 551−559.
(57) Zheng, X.; Huang, T.; Pan, Y.; Wang, W.; Fang, G.; Ding, K.; Wu, M. Enhancing the High-Voltage Cycling Performance of $LiNi_{1/3}Co_{1/3}Mn_{1/3}O_2$/Graphite Batteries Using Alkyl 3,3,3-Trifluoropropanoate as an Electrolyte Additive. *ACS Appl. Mater. Interfaces* **2017**, *9* (22), 18758−18765.
(58) Zhang, Z.; Hu, L.; Wu, H.; Weng, W.; Koh, M.; Redfern, P. C.; Curtiss, L. A.; Amine, K. Fluorinated Electrolytes for 5 V Lithium-Ion Battery Chemistry. *Energy Environ. Sci.* **2013**, *6* (6), 1806−1810.
(59) Achiha, T.; Nakajima, T.; Ohzawa, Y.; Koh, M.; Yamauchi, A.; Kagawa, M.; Aoyama, H. Electrochemical Behavior of Nonflammable Organo-Fluorine Compounds for Lithium Ion Batteries. *J. Electrochem. Soc.* **2009**, *156* (6), A483−A488.
(60) Chen, L.; Fan, X.; Hu, E.; Ji, X.; Chen, J.; Hou, S.; Deng, T.; Li, J.; Su, D.; Yang, X.; Wang, C. Achieving High Energy Density through Increasing the Output Voltage: A Highly Reversible 5.3 V Battery. *Chem.* **2019**, *5* (4), 896−912.
(61) von Aspern, N.; Röschenthaler, G.-V.; Winter, M.; Cekic-Laskovic, I. Fluorine and Lithium: Ideal Partners for High-Performance Rechargeable Battery Electrolytes. *Angew. Chem., Int. Ed.* **2019**, *58* (45), 15978−16000.
(62) Sasaki, Y.; Takehara, M.; Watanabe, S.; Oshima, M.; Nanbu, N.; Ue, M. Electrolytic Behavior and Application to Lithium Batteries of Monofluorinated Dimethyl Carbonate. *Solid State Ionics* **2006**, *177* (3), 299−303.
(63) Xu, K. Electrolytes and Interphases in Li-Ion Batteries and Beyond. *Chem. Rev.* **2014**, *114* (23), 11503−11618.
(64) Kim, C.-K.; Kim, K.; Shin, K.; Woo, J.-J.; Kim, S.; Hong, S. Y.; Choi, N.-S. Synergistic Effect of Partially Fluorinated Ether and Fluoroethylene Carbonate for High-Voltage Lithium-Ion Batteries with Rapid Chargeability and Dischargeability. *ACS Appl. Mater. Interfaces* **2017**, *9* (50), 44161−44172.
(65) Liao, L.; Cheng, X.; Ma, Y.; Zuo, P.; Fang, W.; Yin, G.; Gao, Y. Fluoroethylene Carbonate as Electrolyte Additive to Improve Low Temperature Performance of $LiFePO_4$ Electrode. *Electrochim. Acta* **2013**, *87*, 466−472.
(66) Markevich, E.; Salitra, G.; Fridman, K.; Sharabi, R.; Gershinsky, G.; Garsuch, A.; Semrau, G.; Schmidt, M. A.; Aurbach, D. Fluoroethylene Carbonate as an Important Component in Electrolyte Solutions for High-Voltage Lithium Batteries: Role of Surface Chemistry on the Cathode. *Langmuir* **2014**, *30* (25), 7414−7424.
(67) Markevich, E.; Salitra, G.; Aurbach, D. Fluoroethylene Carbonate as an Important Component for the Formation of an Effective Solid Electrolyte Interphase on Anodes and Cathodes for Advanced Li-Ion Batteries. *ACS Energy Lett.* **2017**, *2* (6), 1337−1345.
(68) Shin, H.; Park, J.; Sastry, A. M.; Lu, W. Effects of Fluoroethylene Carbonate (FEC) on Anode and Cathode Interfaces at Elevated Temperatures. *J. Electrochem. Soc.* **2015**, *162* (9), A1683−A1692.
(69) Liu, B.; Li, B.; Guan, S. Effect of Fluoroethylene Carbonate Additive on Low Temperature Performance of Li-Ion Batteries. *Electrochem. Solid-State Lett.* **2012**, *15* (6), A77−A79.
(70) Ma, L.; Glazier, S. L.; Petibon, R.; Xia, J.; Peters, J. M.; Liu, Q.; Allen, J.; Doig, R. N. C.; Dahn, J. R. A Guide to Ethylene Carbonate-Free Electrolyte Making for Li-Ion Cells. *J. Electrochem. Soc.* **2017**, *164* (1), A5008−A5018.

https://dx.doi.org/10.1021/acsenergylett.0c00643
ACS Energy Lett. 2020, 5, 1438−1447

(71) Suo, L.; Borodin, O.; Gao, T.; Olguin, M.; Ho, J.; Fan, X.; Luo, C.; Wang, C.; Xu, K. Water-in-Salt" Electrolyte Enables High-Voltage Aqueous Lithium-Ion Chemistries. *Science* **2015**, *350* (6263), 938−943.
(72) Ueno, K.; Yoshida, K.; Tsuchiya, M.; Tachikawa, N.; Dokko, K.; Watanabe, M. Glyme−Lithium Salt Equimolar Molten Mixtures: Concentrated Solutions or Solvate Ionic Liquids? *J. Phys. Chem. B* **2012**, *116* (36), 11323−11331.
(73) Yoshida, K.; Nakamura, M.; Kazue, Y.; Tachikawa, N.; Tsuzuki, S.; Seki, S.; Dokko, K.; Watanabe, M. Oxidative-Stability Enhancement and Charge Transport Mechanism in Glyme−Lithium Salt Equimolar Complexes. *J. Am. Chem. Soc.* **2011**, *133* (33), 13121−13129.
(74) He, M.; Su, C.-C.; Peebles, C.; Feng, Z.; Connell, J. G.; Liao, C.; Wang, Y.; Shkrob, I. A.; Zhang, Z. Mechanistic Insight in the Function of Phosphite Additives for Protection of $LiNi_{0.5}Co_{0.2}Mn_{0.3}O_2$ Cathode in High Voltage Li-Ion Cells. *ACS Appl. Mater. Interfaces* **2016**, *8* (18), 11450−11458.
(75) Liao, B.; Xu, M.; Hong, P.; Li, H.; Wang, X.; Zhu, Y.; Xing, L.; Li, W. Enhancing Electrochemical Performance of $Li/LiMn_2O_4$ Cell at Elevated Temperature by Tailoring Cathode Interface via Diethyl Phenylphosphonite (DEPP) Incorporation. *J. Appl. Electrochem.* **2017**, *47* (10), 1161−1172.
(76) Zheng, X.; Wang, X.; Cai, X.; Xing, L.; Xu, M.; Liao, Y.; Li, X.; Li, W. Constructing a Protective Interface Film on Layered Lithium-Rich Cathode Using an Electrolyte Additive with Special Molecule Structure. *ACS Appl. Mater. Interfaces* **2016**, *8* (44), 30116−30125.
(77) Lux, S. F.; Lucas, I. T.; Pollak, E.; Passerini, S.; Winter, M.; Kostecki, R. The Mechanism of HF Formation in $LiPF_6$ Based Organic Carbonate Electrolytes. *Electrochem. Commun.* **2012**, *14* (1), 47−50.
(78) Fan, X.; Chen, L.; Ji, X.; Deng, T.; Hou, S.; Chen, J.; Zheng, J.; Wang, F.; Jiang, J.; Xu, K.; Wang, C. Highly Fluorinated Interphases Enable High-Voltage Li-Metal Batteries. *Chem.* **2018**, *4* (1), 174−185.
(79) Adams, B. D.; Zheng, J.; Ren, X.; Xu, W.; Zhang, J.-G. Accurate Determination of Coulombic Efficiency for Lithium Metal Anodes and Lithium Metal Batteries. *Adv. Energy Mater.* **2018**, *8* (7), 1702097.
(80) Edström, K.; Gustafsson, T.; Thomas, J. O. The Cathode−Electrolyte Interface in the Li-Ion Battery. *Electrochim. Acta* **2004**, *50* (2), 397−403.
(81) Jiao, S.; Ren, X.; Cao, R.; Engelhard, M. H.; Liu, Y.; Hu, D.; Mei, D.; Zheng, J.; Zhao, W.; Li, Q.; Liu, N.; Adams, B. D.; Ma, C.; Liu, J.; Zhang, J.-G.; Xu, W. Stable Cycling of High-Voltage Lithium Metal Batteries in Ether Electrolytes. *Nat. Energy* **2018**, *3* (9), 739.
(82) Cui, W.; Lansac, Y.; Lee, H.; Hong, S.-T.; Jang, Y. H. Lithium Ion Solvation by Ethylene Carbonates in Lithium-Ion Battery Electrolytes, Revisited by Density Functional Theory with the Hybrid Solvation Model and Free Energy Correction in Solution. *Phys. Chem. Chem. Phys.* **2016**, *18* (34), 23607−23612.
(83) Borodin, O.; Olguin, M.; Ganesh, P.; Kent, P. R. C.; Allen, J. L.; Henderson, W. A. Competitive Lithium Solvation of Linear and Cyclic Carbonates from Quantum Chemistry. *Phys. Chem. Chem. Phys.* **2016**, *18* (1), 164−175.
(84) Chen, X.; Zhang, X.-Q.; Li, H.-R.; Zhang, Q. Cation−Solvent, Cation−Anion, and Solvent−Solvent Interactions with Electrolyte Solvation in Lithium Batteries. *Batteries & Supercaps.* **2019**, *2* (2), 128−131.

https://dx.doi.org/10.1021/acsenergylett.0c00643
ACS Energy Lett. 2020, 5, 1438−1447